ELSEVIER

Biophysical Chemistry 86 (2000) 95–108

Biophysical Chemistry

www.elsevier.nl/locate/bpc

Gamma S-crystallin of bovine and human eye lens: solution structure, stability and folding of the intact two-domain protein and its separate domains ☆

Martina Wenk[a], Ruth Herbst[a], Dagmar Hoeger[a], Michael Kretschmar[a], Nicolette H. Lubsen[b], Rainer Jaenicke[a,*]

[a] *Institute of Biophysics and Physical Biochemistry, University of Regensburg, D-93040 Regensburg, Germany*
[b] *Department of Biochemistry, University of Nijmegen, 6525ED Nijmegen, The Netherlands*

Received 4 November 1999; accepted 3 February 2000

Abstract

Human and bovine γS-crystallin (HγS and BγS) and their isolated N- and C-terminal domains were cloned and expressed as recombinant proteins in *E. coli.* HγS and BγS are found to be authentic according to their spectral and hydrodynamic properties. Both full-length proteins and isolated domains are monomeric and exhibit high thermal and pH stabilities. The thermodynamic characterization made use of chemically and thermally-induced equilibrium unfolding transitions at varying pH. In spite of its exemplary two-domain structure, γS-crystallin does not show bimodal unfolding characteristics. In the case of BγS, at pH 7.0, the C-terminal domain is less stable than the N-terminal one, whereas for HγS the opposite holds true. Differential scanning calorimetry confirms the results of chemically-induced equilibrium unfolding transitions. Over the whole pH range between 2.0 and 11.5, HγS-crystallin and its isolated domains (HγS-N and HγS-C) follow the two-state model. The two-state unfolding of the intact two-domain protein points to the close similarity of the stabilities of the constituent domains. Obviously, interactions between the domains do not contribute significantly to the overall stability of γS-crystallin. In contrast, the structurally closely related γB-crystallin owes much of its extreme stability to domain interactions.

Keywords: Crystallins; Differential scanning calorimetry; Protein folding; Protein stability; Domain interaction

☆ Dedicated to Professor Heini Eisenberg, mentor and friend.

* Corresponding author. Tel.: +49-941-943-3015; fax: +49-941-943-2813.
E-mail address: rainer.jaenicke@biologie.uni-regensburg.de (R. Jaenicke).

0301-4622/00/$ - see front matter
PII: S0301-4622(00)00161-7

1. Introduction

The eye lens is a multilayer epithelial syncytium which allows focusing objects on the retina. It maintains transparency without significant turnover of its constituent proteins over the whole life-time of an organism. During terminal development, the fiber cells of the lens are mere non-compartmentalized containers filled with a species-specific and age-dependent mixture of proteins, called *crystallins*, at a concentration of up to 700 mg/ml. It is just the close packing and well-defined short-range order of the crystallins which allow the eye lens to fulfil its function with minimal perturbations by light scattering and optical aberrations [1]. Among the 'ubiquitous' αβγ-crystallins, the βγ-superfamily of proteins is the abundant structural protein in vertebrate eye lens. It forms a class of homologous two-domain proteins with the two Greek-key motif of four-stranded antiparallel β-sheets as the common topology [2,3].

γS-crystallin is the main protein component in the human eye lens [4]. It represents an early branch of the γ-crystallin family which has been conserved throughout evolution, indicating an essential function in the eye. Since its expression only starts postpartum [5,6], it is compartmentalized in the water-rich cortex. In contrast, γB-crystallin is specialized for a low-water content and accumulates mainly in the dehydrated glassy lens nucleus [7]. Based upon its chromatographic behavior, γS was first classified as a β-crystallin (βS-crystallin). However, its gene organisation and sequence clearly place it within the γ-crystallin family [8–11].

Crystallization of native γS-crystallin has not been achieved so far. Therefore, the close phylogenetic relationship between γB and γS has been used to construct a three-dimensional model of human γS by homology modeling, based on the known spatial structures of bovine γB- and γB2-crystallin [12]. The model predicts that γS, apart from an (5-residues) N-terminal extension, differs from γB mainly in the interface region between the domains. The charged residues are generally paired in a different way from both parental structures, γB and γB2, thus allowing the different roles of γB and γS in the eye lens to be correlated with specific physical properties. The hypothetical spatial structure still awaits its experimental verification. With respect to their solution properties, γB and γS exhibit very similar hydrodynamic characteristics, however, γS seems to be distinct from the other γ-crystallins by different gel-filtration and phase-separation properties as well as lower stability [12–15]. To understand the structural correlates of these physical properties, in the present study a detailed study of γS-crystallin was undertaken. Because of its predominant role in the human eye lens, special emphasis was put on HγS. However, the comparison of γS and γB will also include the bovine protein and its domains, especially an extension-less mutant with the five N-terminal amino acid residues missing. The truncation brings γS closer to γB which lacks the extension of wild-type γS, stressing the relationship between the two crystallins [16].

2. Materials and methods

2.1. Materials

Bacto yeast extract and Bacto trypton for media were purchased from Difco Laboratories (Detroit, MI, USA), guanidinium chloride (GdmCl) and urea (U), *ultra pure*, from ICN/Schwarz-Mann (Cleveland, OH, USA), and dithiothreitol (DTT) from Biomol (Hamburg, Germany). Other chemicals were A-grade from Merck (Darmstadt, Germany); solutions were made up from doubly-destilled water.

2.2. Cloning

The full-length calf γS-crystallin cDNA clone and the N-terminal domain were cloned in the *pET3a* vector essentially as described for the C-terminal domain of calf γS-crystallin [17]. In short, the desired coding sequence was isolated by PCR, using primers containing an NdeI site at the initiation codon and a *Bam*HI site 3′ of the stop codon. PCR products were cloned in a pGEM-T vector (Promega) and sequenced. NdeI/*Bam*HI

fragments were then excised and cloned in the *pET3a* vector. The full-length human γS sequence was amplified from a human lens cDNA library in lambda-gt11 using primers designed on the basis of the published γS-crystallin sequence. The PCR products were cloned and sequenced. Expression clones of the full-length cDNA sequence and the separate N- and C-terminal domain were made in *pET3a* using the same approach taken for the calf γS-crystallin clones.

2.3. Expression and purification of the recombinant proteins

BγS, HγS and their isolated domains were expressed in *E. coli* BL21 harboring a *pET3a* expression plasmid, which carried either the BγS or the HγS sequence, or the respective sequences of the isolated domains: 1–91 and 93–177, for BγS-N and BγS-C, or 1–90 and 91–177, for HγS-N and HγS-C. Cells were grown in 2-l LB-medium with 100 μg/ml ampicillin at 37°C. At $OD_{546\ nm}$ = 0.6, isopropyl-ßD-thiogalactoside (IPTG) was added to a final concentration of 1 mM. After a further growth period of 12–16 h, cells were harvested, and the soluble fraction of the cell lysate was dialyzed against 10 mM sodium phosphate at pH 6.0, 1 mM EDTA (buffer A). The lysate was applied to an SP-Sepharose Fast Flow column (Pharmacia, Uppsala, Sweden) in buffer A, and eluted by a linear gradient of 0–0.3 M NaCl. Fractions containing the γS-crystallins or their domains were combined, and ammonium sulfate was added to a final concentration of 2 M. The solution was applied to a Phenyl-Sepharose Fast Flow CL4B column (Pharmacia) in 25 mM sodium phosphate at pH 7.0, 2 M ammonium sulfate, 1 mM EDTA (buffer B), and the protein was eluted by a linear gradient of 2–OM ammonium sulfate. The purified proteins were concentrated by 100% ammonium sulfate precipitation and desalted using a PD10 column (Pharmacia) in 10 mM sodium phosphate pH 7.0, 1 mM EDTA (buffer C). As judged by silver-stained SDS polyacrylamide gels, the proteins were obtained in pure form. For the purification of HγS-C, the purification scheme was the same as described before, except for two points: Instead of buffer A, 25 mM sodium acetate of pH 5.5, 1 mM EDTA (buffer D) was applied, and the domain was eluted directly from the Phenyl-Sepharose Fast Flow CL4B column by 25 mM sodium phosphate of pH 7.0, 1 mM EDTA, 2 M ammonium sulfate (buffer E).

2.4. Protein concentration

Molar extinction coefficients of the proteins were calculated according to Gill and von Hippel [18] and Pace et al. [19]: $A_{280\ nm;\ 0.1\%;\ 1\ cm}$ = 1.98 (HγS), 2.09 (HγS-N), 1.87 (HγS-C) and 1.93 (BγS), 2.0 (BγS-5), 2.09 (BγS-N), 1.8 (BγS-C), respectively.

2.5. Spectroscopy

Absorption spectra were monitored using a Cary 1 UV-vis spectrophotometer with standard 1-cm quartz cells (Hellma, Müllheim, Germany). The band width was set to 1 nm, the data interval to 2 nm, and the integration time to 0.6 s.

Fluorescence emission spectra were recorded in a Spex FluoroMax-2 spectro-fluorometer equipped with a thermostated cell holder and 1-cm semi-micro quartz cells (Hellma). For emission spectra at λ_{exc} = 280 nm, the spectral bandwidths were 3 and 5 nm for excitation and emission, respectively. With an increment of 0.2 nm, the integration time for each point was 1 s.

Near-UV circular dichroism spectra were measured in 1 cm cylindrical cuvettes, far-UV spectra in 0.1 or 1.0 mm cuvettes, making use of an Aviv 62A-DS spectrophotometer. The spectral bandwidth was 1 nm. Spectra, with data points at 0.2 nm intervals and 0.6 s integration time, were accumulated over 16 repeated scans, corrected for solvent background and smoothed using linear interpolation. Thermal unfolding in the presence of various amounts of GdmCl was accomplished by stepwise heating of the samples, from approximately 10 to 100°C at a heating rate of 0.3 K/min, monitoring the absorbance at 286 nm.

2.6. Analytical size exclusion chromatography

To determine the hydrodynamic properties and

the state of association, gel permeation chromatography was applied using a Superdex 75 High Resolution 10/30 column (Pharmacia) at room temperature and a flow rate of 30 ml/h. The column was equilibrated with 10 mM sodium phosphate at pH 7.0, 1 mM EDTA, 5 mM DTT and 200 mM NaCl (buffer F). Protein samples (50 μl) were applied to the column at a final protein concentration of 0.2 or 5 mg/ml. The eluting protein was monitored by UV absorption at 280 nm using a Uvicord SII (LKB Pharmacia Biotech, Uppsala). To calibrate the column, the LMW Gel Filtration Calibration Kit (Amersham Pharmacia Biotech) was used.

2.7. Mass spectrometry and ultracentrifugation

Quantitative determinations of molecular weights made use of mass spectrometry and ultracentrifugation. For mass-spectrometric analyses, electrospray ionization was applied (SSQ Finnigan Mass Spectrometer). Samples in methanol/water (1:1) plus 0.1% acetic acid were injected in positive ion mode.

Sedimentation velocity and high-speed sedimentation equilibrium experiments were performed in a Beckman Model E analytical ultracentrifuge using a high-sensitivity UV scanning system as well as Schlieren optics. 2 and 12-mm double-sector cells with sapphire windows were used in AnG and AnD rotors. Sedimentation coefficients were obtained from velocity runs at 44 000 and 60 000 rev./min, plotting ln r vs. t and correcting for 20°C and water viscosity. Sedimentation equilibria at 24 000 and 12 000 rev./min made use of the meniscus depletion technique [20] at scanning wavelengths of 230, 280, 290 and 300 nm. Weight-average molecular weights were evaluated from ln c vs. r^2 plots making use of computer programs kindly provided by Drs G. Böhm (University of Halle-Wittenberg) and A. Minton (NIH, Bethesda). The partial specific volumes were calculated from the amino acid composition. Proteins were dissolved in 10 mM sodium phosphate buffer of pH 7.0, 1 mM EDTA and 2 mM DTT; protein concentrations: 0.7–2.0 mg/ml.

2.8. Equilibrium unfolding and refolding

GdmCl- and urea-induced unfolding were measured in 10 mM sodium phosphate at pH 7.0, 1 mM EDTA, 5 mM DTT (buffer G). To study refolding, samples were denatured in 5 M GdmCl or 10 M urea, and subsequently diluted into buffer G, containing varying amounts of the corresponding denaturant. For equilibrium measurements, samples were incubated at 20°C for 24–32 h. Equilibration was followed either by fluorescence emission at the maximal difference of intrinsic fluorescence between the native and denatured states (320 and 360 nm), or by the change in the far-UVCD signal at 220 nm.

2.9. Differential scanning calorimetry

DSC studies were performed using a Nano-DSC CSC 5100 calorimeter (Calorimetry Sciences Corp., Provo, UT, USA). All experiments were carried out in 20 mM glycine/HCl, of pH 2.0–3.0 at protein concentrations between 0.8 and 1.5 mg/ml. Samples were dialyzed against a 1000-fold volume of buffer. Buffers were filtrated and degassed by evacuation; protein solutions were filtrated and degassed before the concentration was determined by absorption spectroscopy. Baselines and samples were measured under identical conditions. To examine the reversibility of folding, the protein was cooled down after the first unfolding transition, and heated up a second time. Data were analyzed with the deconvolution software CpCalc 2.1 of the CSC 5100 [21], using specific partial volumes of 0.72 (HγS), 0.71 (HγS-N) and 0.73 (HγS-C).

ΔC_P was determined by plotting ΔH vs. T_M according to the Kirchhoff equation. The slopes of the linear regression lines allow the calculation of ΔC_P. Gibbs free energies of unfolding were determined making use of the following equation:

$$\Delta G(T) = \Delta H(T_M) * [(T_M - T)/T_M] - \Delta Cp * (T_M - T) + \Delta Cp * T * \ln(T_M/T).$$

2.10. Kinetic experiments

Folding and unfolding kinetics were monitored using fluorescence ($\lambda_{exc} = 280$ nm, $\lambda_{em} = 360$ nm) for HγS and HγS-C, and absorbance (286 nm) for HγS and HγS-N (Spex Fluoromax-2 spectrophotometer and Cary 1/3 Varian spectrophotometer). All experiments were carried out in 10 mM sodium phosphate, 1 mM EDTA, 5 mM DTT, of pH 7.0 at 20°C. Unfolding and refolding were accomplished by dilution with solutions varying in GdmCl concentration. Final protein concentrations: 0.2 mg/ml (absorption) and 0.005 mg/ml (fluorescence) for HγS, 0.2 mg/ml for HγS-N, and 0.01 mg/ml for HγS-C. The individual kinetics were analyzed as mono-exponential or double-exponential functions.

3. Results

3.1. Cloning, expression and purification

Recombinant BγS, BγS-5, HγS and their N- and C-terminal domains BγS-N, BγS-C, HγS-N and HγS-C were cloned and heterologously expressed in *E. coli* as described in Section 2. Their physico-chemical characterization is summarized in Table 1. As taken from the mass-spectrometric data and the N-terminal sequences, the molecular masses are in agreement with the calculated values based on the published primary structures, thus providing strong evidence for the authenticity of the recombinant proteins.

3.2. Molecular masses and assembly properties

Analytical gel permeation chromatography of all seven proteins in the presence of 5 mM DTT and at concentrations between 0.2 and 5 mg/ml yields elution volumes corresponding to the molecular masses of the monomers. The sedimentation analysis in the analytical ultracentrifuge at concentrations up to 5 mg/ml confirms this conclusion with high precision (Table 1). However, analyzing the molecular weight distribution carefully, there is an obvious difference between bovine and human γS. The 1:1 BγS(N + C) mixture shows a tendency to form a heterodimer, whereas in the case of HγS(N + C), in the given concentration range no 'nicked' form of HγS is observed. Due to the low association constant (< 3 mM), the domain interactions are undetectable by spectroscopic methods.

Table 1
Molecular characteristics and mass determination of BγS- and HγS-crystallin and their N- and C-terminal domains

Protein	Residues	M^{a}_{calc} [Da]	M^{a}_{MS} [Da]	pI[b]	$s_{20,w}$ [c] [S]	M^{c}_{HSSE} [Da]
BγS	177(S1-E177)	20796	–	6.4	2.52 ± 0.06	21400 + 1120
BγS-5	172(K6-E177)	20352	–	–	2.48 ± 0.06	20870 ± 1400
BγS-N	91(S1-G91)	10513	–	–	1.54 ± 0.06	10740 ± 770
BγS-C	85(Y93-E177)	10174	–	–	1.50 ± 0.03	12370 ± 600
BγS(N + C)	–	–	–	–	1.95 ± 0.06[d]	14500 ± 2000[e]
HγS	177(S1-E177)	20876	20873	6.4	2.54 ± 0.08	22110 ± 1530
HγS-N	90(S1-G90)	10480	10480	6.7	1.57 ± 0.10	10990 ± 1010
HγS-C	87(G91-E177)	10413	10410	6.1	1.54 ± 0.08	10710 ± 380
HγS(N + C)	–	–	–	–	1.64 ± 0.08[d]	10180 ± 560

[a] Molecular masses M_{calc} and M_{MS} calculated by the program ExPASy and by electrospray mass spectrometry, respectively.
[b] Calculated isoelectric point.
[c] $s_{20,w}$ and M_{HSSE} refer to the sedimentation coefficient at 0.2 mg/ml, and to the molecular masses from high-speed sedimentation equilibria, respectively. Scanning wavelength: 280 nm.
[d] Sedimentation analysis of a 1:1 mixture of the N- and C-terminal domains at 2 mg/ml.
[e] Fitting the A vs. r profiles according to a monomer-heterodimer equilibrium (using the Minton program); for the BγS-domains an association constant of approximately 3 mM is obtained.

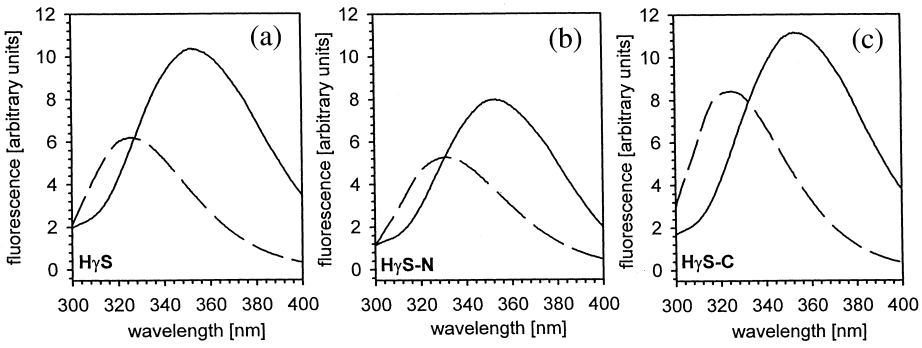

Fig. 1. Fluorescence emission spectra of (a) HγS, (b) HγS-N and (c) HγS-C in 10 mM sodium phosphate, 1 mM EDTA, 5 mM DTT, pH 7.0, 20°C; native (---) and unfolded in 6 M GdmCl (—). Protein concentration: 50 μg/ml; $\lambda_{exc.} = 280$ nm.

3.3. Spectroscopy

The spectroscopic properties of bovine and human γS are determined by their relatively high tryptophan and tyrosine content: 4 Trp (2 in each domain), and more than 10 Tyr (again more or less equally distributed). The 9 and 10 Phe residues contribute significantly only to the region between 250 and 260 nm. Maximum absorbance is observed at 278 nm, with a second slightly lower peak at 282 nm, both attributable to Trp and Tyr; a marked shoulder at 290 nm is mainly caused by Trp. Upon denaturation in 6 M GdmCl (pH 7.0), the amplitudes are marginally decreased, showing a slight blue-shift of the 278 nm peak to 277 nm and flattening of the second maximum and the shoulder at 290 nm. The corresponding difference spectra of the native and the unfolded states exhibit two maxima at 286 and 293 nm. Due to the large number of aromatic residues and the high symmetry of the two-domain structure, the given characteristics hold to a good approximation for the two homologous full-length proteins and their domains (data not shown).

In fluorescence, the previous subtle absorption changes are magnified; Fig. 1 illustrates the dramatic red-shifts and the increases in emission, using the human proteins as examples. Evidently, the exposure of aromatic residues to the aqueous solvent upon unfolding releases the quench, especially of the Trp residues, allowing the 'intrinsic markers' to be used to monitor folding/unfolding transitions both in equilibrium and kinetic experi-

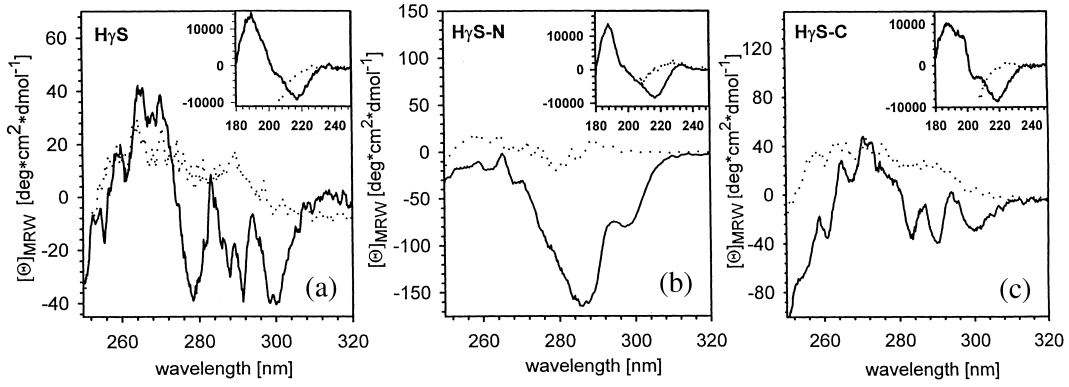

Fig. 2. Near-UV CD spectra of (a) HγS, (b) HγS-N and (c) HγS-C in 10 mM sodium phosphate, 1 mM EDTA, 5 mM DTT, pH 7.0, 20°C; native (—) and unfolded in 6 M GdmCl (·). Protein concentration: 0.8 mg/ml. Inset: Far-UV CD spectra.

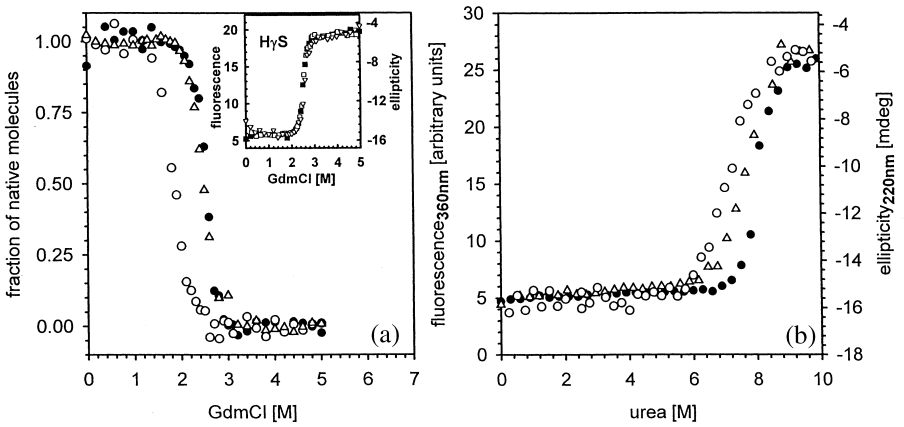

Fig. 3. (a) Normalized GdmCl-induced and (b) urea-induced equilibrium transitions of (●) HγS, (○) HγS-N and (△) HγS-C at pH 7.0 and 20°C monitored by fluorescence at 360 nm and far-UV CD at 220 nm, respectively. Buffer: 10 mM sodium phosphate, 1 mM EDTA, 5 mM DTT, pH 7.0. Protein concentration: HγS: 10 μg/ml (fluorescence), 200 μg/ml (far-UV CD); HγS-N: 200 μg/ml (far-UV CD); HγS-C: 10 μg/ml (fluorescence). Inset: HγS (■) unfolding and (□) refolding detected by fluorescence and (▽) unfolding detected by far-UV CD.

ments. The near-UV CD may serve the same purpose; on the other hand, alterations in the far-UV CD reflect the destruction or formation of secondary structure. Results for the native and unfolded proteins in Fig. 2 prove the spectral characteristics of the different proteins to be closely similar.

3.4. Stability

The high long-term stability of the protein components of the vertebrate eye lens is an intriguing property that needs a biophysical explanation. In the present context, the easiest way to collect thermodynamic data would be thermal denaturation making use of calorimetry. However, even at low protein concentration, absorbance and CD measurements have shown that at pH 7.0 the unfolding reaction is irreversible. There are two ways out of the dilemma: (i) equilibrium unfolding transitions using chemical denaturation by chaotropic agents such as GdmCl or urea; and (ii) optimization of the denaturation conditions by altering the solvent parameters. The combination of both approaches has often turned out to be useful not only in accomplishing full reversibility but also in investigating the folding mechanism. To give an example, changing from GdmCl- to urea-denaturation at low pH, allowed independent domain folding to be established in the case of BγB-crystallin [22,23].

In the present study, the stability of γS-crystallin was characterized by pH-, GdmCl-, urea- and temperature-induced denaturation, measuring changes in absorbance, fluorescence emission and dichroic absorption. In the case of bovine γS and its domains, protonation/deprotonation at pH 2.0–11.5 apparently did not affect the conformation, i.e. no changes were observed in absorbance, fluorescence and CD. For BγB, the same results were obtained [3,23]. At pH 12, the spectral data clearly point to significant unfolding: A_{max} is found to be shifted from 278 to 288 nm, F_{max} from 325 to 354 nm, and the CD signal is flattened over the whole wavelength range between 320 and 215 nm (data not shown).

Since denaturation at high pH is difficult to interpret, GdmCl- and urea-induced equilibrium unfolding transitions at neutral pH were applied in order to quantify the intrinsic stabilities of BγS, BγS-5, HγS and their domains (Fig. 3). The numerical data (Table 2) allow the following conclusions to be drawn: (i) chemical denaturation leads to fully reversible unfolding/refolding transitions; (ii) the equilibria monitored by different

Table 2
Midpoints of the GdmCl- and urea-induced equilibrium transitions of human and bovine γS-crystallin and their isolated domains in 10 mM sodium phosphate[a]

Protein	$C_{1/2\,[GdmCl]}$ [M]	$C_{1/2\,[urea]}$ [M]
BγS	2.1[b]	7.0[b]
BγS-5	2.1[b]	7.4[b]
BγS-N	1.8[b]	6.6[b]
BγS-C	1.8[b]	6.0[b]
HγS	2.6[b,c]	8.0[b]
HγS-N	1.9[c]	7.0[c]
HγS-C	2.5[b]	7.6[b]

[a] pH 7.0, 1 mM EDTA, 5 mM DTT.
[b] Detected by fluorescence at 360 nm; range of error: ±0.1 M.
[c] Detected by far-UV CD at 220 nm; range of error: ±0.1 M.

spectral techniques coincide, suggesting two-state behavior for all seven proteins; and (iii) the intrinsic stabilities of BγS, BγS-5, HγS and their constituent domains are extremely high; for all three, the stabilities of the complete two-domain proteins exceed the stabilities of the domains. However, in BγS the C-domain is less stable than the N-domain and BγS itself; in HγS the opposite holds true. Compared to BγS, BγS-5 exhibits a slightly increased stability.

3.5. Thermal transitions

In contrast to the bimodal unfolding observed in the case of bovine γB-crystallin [23], bovine and human γS-crystallin show no indication for independent domain folding; no intermediate with one domain unfolded and the other still intact could be detected. Basically for all equilibrium unfolding transitions of BγS, HγS and their isolated domains, the two-state model was sufficient to fit the experimental data. The reason for the anomalous behaviour may be the differences in net charge Δz of the two domains at low pH: it is 3 for γB, whereas in the case of γS, it is only 1 [24]. As a consequence, HγS and its isolated domains are native at pH 2 (Fig. 4).

At neutral pH, the thermal analysis of HγS was hampered by the high stability of the protein. The denaturation kinetics were found to be extremely slow; and the protein aggregated at concentrations > 0.1 mg/ml; beyond 80°C, the protein underwent chemical modification. For the given reasons, two approaches were combined in order to obtain thermodynamic data for HγS-crystallin and its domains at physiological pH. First, at 50 μg/ml, thermal unfolding (followed by absorbance) was found to be reversible in the presence of up to 2 M GdmCl; under this condition, all melting profiles were monophasic, allowing the

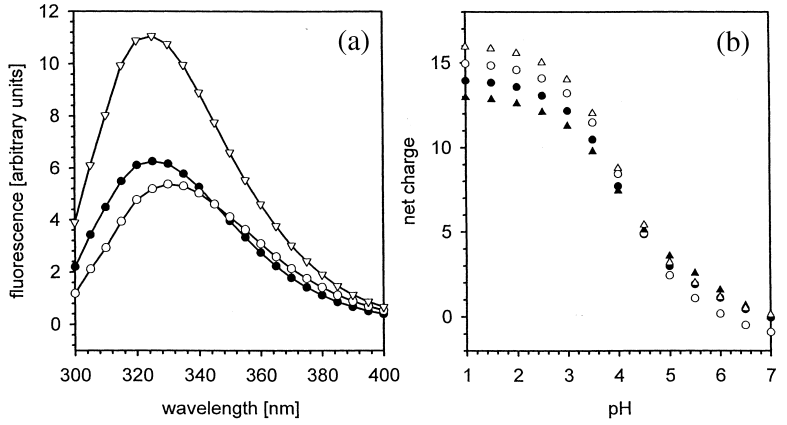

Fig. 4. (a) Fluorescence emission spectra of (▽) HγS, (○) HγS-N and (●) HγS-C in 20 mM glycine/HCl, pH 2.0, 20°C. $\lambda_{exc.} = 280$ nm. Protein concentration: 20 μg/ml. (b) Comparison of the net charges of the domains from BγB- and BγS-crystallin in dependence on pH. (△) BγBC, (▲) BγBN, (○) HγS-C and (●) HγS-N. Calculated using the published sequences of γB- and γS-crystallin and software provided in www.embl-heidelberg.de.

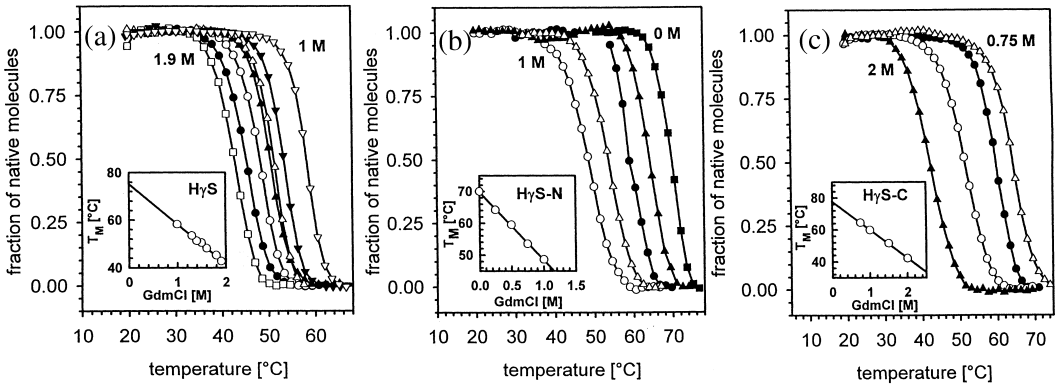

Fig. 5. Normalized thermal transitions of (a) HγS, (b) HγS-N and (c) HγS-C in 10 mM sodium phosphate, 1 mM EDTA, 5 mM DTT, pH 7.0 at varying GdmCl-concentrations, detected by absorbance at 286 nm. Protein concentration: 50 μg/ml; heating rate: 0.3 K/min. Inset: T_M vs. [GdmCl] plots with extrapolation to zero GdmCl concentration.

determination of T_M at zero GdmCl concentration by linear extrapolation (Fig. 5; Table 3). Second, at pH 2–3, reversible unfolding was accomplished at protein concentrations as high as 1.5 mg/ml; thus, thermal analysis by differential scanning calorimetry was feasible (cf. Table 3). As shown in Fig. 6, repeated scanning yielded $> 90\%$ reversibility, permitting deconvolution according to the two-state model. Linear Kirchhoff plots of the ΔH_M^-vs. ΔT_M^-values allow the molar heat capacity change ΔC_P to be calculated. Assuming ΔC_P to be independent of temperature, the extrapolated T_M at pH 7 from thermal unfolding (Fig. 5) may be used to determine ΔH_M at neutral pH (insets, Fig. 6). Combining the thermodynamic parameters, the Gibbs free energies of stabilization were calculated for HγS and its domains at physiological pH (Table 3). The stability profiles (corrected for the molecular masses) reveal a slightly decreased stability of HγS-N compared to HγS-C, as observed also for the GdmCl- and urea-induced unfolding transitions; however, the deviations are small and the stability profiles of all three proteins closely similar (Fig. 7). The two domains exhibit nearly identical stabilities explaining the monophasic two-state unfolding of the complete two-domain HγS molecule. Evidently, the contribution of domain interactions to

Table 3
Thermodynamic stability of HγS-crystallin and its isolated domains at pH 7.0

	HγS	HγS-N	HγS-C
ΔC_P [kJ/(mol* K)][a]	7.5 ± 1	3.5 ± 0.5	4.5 ± 0.5
$T_{M,\ \mathrm{pH\ 7.0,\ H_2O}}$ [°C][b]	75 ± 1	70 ± 1	78 ± 1
$\Delta H_{M,\ \mathrm{pH\ 7.0}}$ [kJ/mol][c]	750 ± 20	380 ± 10	430 ± 10
$\Delta G_{\mathrm{pH\ 7.0,\ 20°C}}$ [kJ/mol][d]	84 ± 10	42 ± 5	48 ± 5
$\Delta G_{\mathrm{pH\ 7.0,\ 20°C}}$ [J/g][d]	4.0 ± 0.5	4.0 ± 0.5	4.5 ± 0.5

[a] ΔC_P: molar heat capacity change determined by a Kirchhoff plot using calorimetrically measured T_M and ΔH_M at pH 2.0-3.0 (Fig. 6).

[b] $T_{M,\ \mathrm{pH\ 7.0,\ H_2O}}$: melting point at pH 7.0 in H_20, determined from linear extrapolation of the melting points of thermal transitions at pH 7.0 in the presence of various amounts of GdmCl to aqueous solution (Fig. 5).

[c] $\Delta H_{M,\ \mathrm{pH\ 7.0}}$: Enthalpy change at pH 7.0 determined from the extrapolation of the linear regression of ΔC_P (assumed to be constant) to the melting point at pH 7.0 (Fig. 6).

[d] $\Delta G_{\mathrm{pH\ 7.0,\ 20°C}}$: Gibbs free energies at pH 7.0 and 20°C in [kJ/mol] and corrected for the molecular masses (Table 1) in [J/g], respectively.

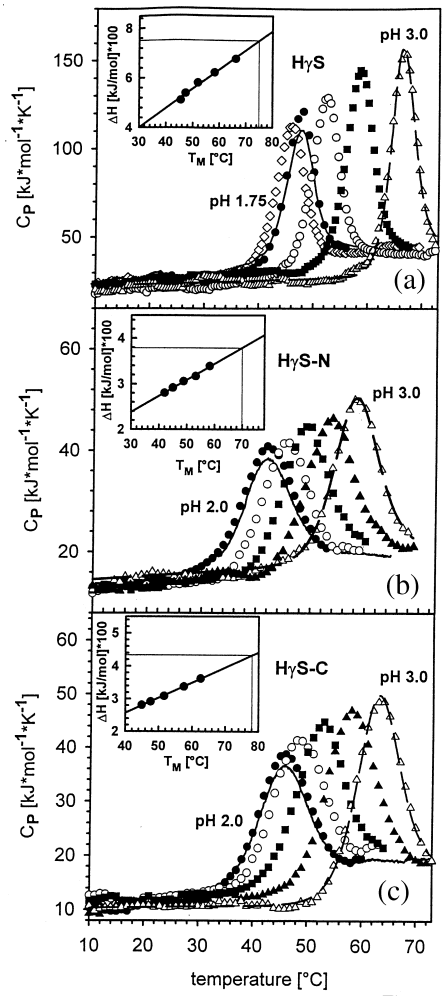

Fig. 6. DSC-scans of (a) HγS, (b) HγS-N and (c) HγS-C in 20 mM glycine/HCl, pH 1.75–3.0. (—) second heating to check for reversibility; (---) fit of the data according to the two-state model. Heating rate: 0.25 K/min. Protein concentration: 0.8–1.5 mg/ml. Insets: ΔH_M vs. T_M plots with linear regression for the calculation of ΔC_P and the determination of ΔH_M, using T_M at pH 7.0, extrapolated from thermal and GdmCl-induced unfolding transitions (cf. Fig. 5).

the overall stability of the intact molecule is small, its Gibbs free energy lies in the range of error.

3.6. Folding kinetics

Under equilibrium conditions, HγS and its isolated domains obey the two-state model without detectable equilibrium intermediates. In contrast, unfolding/refolding kinetics give clear evidence for *kinetic* intermediates on the folding pathway: While unfolding for all three proteins was monophasic, refolding revealed biphasic kinetics for HγS, and strong 'roll-over' effects [25] for all three proteins at low GdmCl concentrations (Fig. 8). Temporal separation of domain folding and pairing or intermediates with wrong proline conformation may be the reason for the observed non-linearity. The latter could be excluded by double-jump experiments [26], monitoring the kinetics of refolding after varying unfolding times (data not shown).

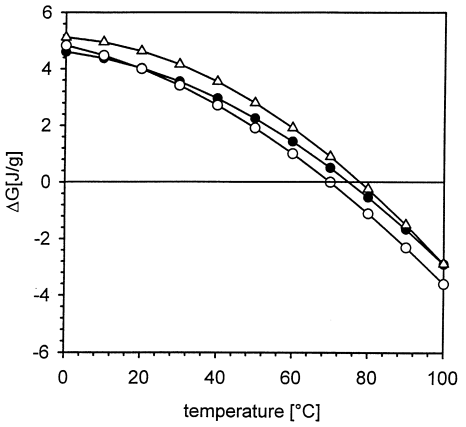

Fig. 7. Gibbs free energy ΔG [J/g] as a function of temperature at pH 7.0: (●) HγS, (○) HγS-N and (△) HγS-C.

4. Discussion

The γ-crystallin superfamily of eye lens proteins has two branches, one with multiple members in mammals organized in a six-gene cluster (γA to γF), and one with γS as the only member [7]. The latter is ubiquitous in vertebrates and exhibits extremely high structural homology, with 93% sequence identity, between the bovine and the human protein [10]. As an explanation for the difference in variability it was proposed that the six-gene cluster is specifically adapted to the dehydrated environment of the lens nucleus (a property variable between species), whereas γS is found in the ubiquitously present water-rich cortical region of the eye lens.

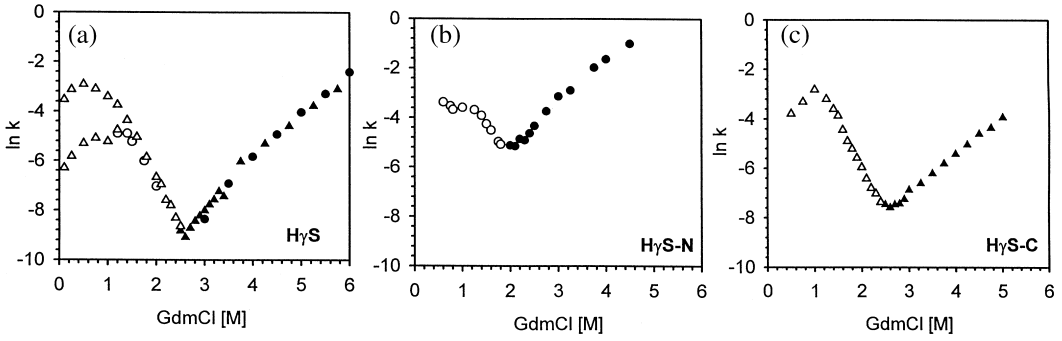

Fig. 8. Dependence of the apparent rate constant k on GdmCl concentration for (a) HγS, (b) HγS-N, and (c) HγS-C in 10 mM sodium phosphate, 1 mM EDTA, 5 mM DTE, pH 7.0, 20°C. Protein concentration: 0.2 and 0.005 mg/ml for HγS, 0.2 mg/ml for HγS-N, and 0.01 mg/ml for HγS-C. Method of detection: Refolding: (△) fluorescence, (○) absorbance. Unfolding: (▲) fluorescence, (●) absorbance.

In comparing γS-crystallin from calf and man, it becomes clear that earlier data collected for bovine γS [12–14,27] also hold for the human protein. As one would predict, the high sequence identity corresponds to a close similarity of the structural parameters of both proteins in solution: All spectral properties are qualitatively identical, and even in quantitative terms, the differences are small. Although still no high-resolution structure of complete γS-crystallin is available, evidence from the coordinates of the C-terminal domain [17] leaves no doubt that the topology of the full-length protein must be closely related to the two-domain organisation of γB-crystallin. The fact that the isolated domains γS-N and γS-C can be expressed and purified as stable entities with properties similar to those of the domains of γB clearly corroborates this view.

For γB- and γβ2-crystallin and their isolated domains and assemblies, X-ray coordinates are available to a resolution of better than 2 Å [2,3,28,29]. They allowed a three-dimensional model of γS to be predicted. The result suggested a difference between γB and γS mainly in the interface region between the domains, where the charged residues were found to be paired in a different way from both β- and γ-crystallins [12]. Possibly it is this difference that allows 'nicked γS' to be formed, whereas for βγ-crystallins no association tendency of the isolated domains has been discovered, unless they were truncated either at their extensions or termini [30,31]. The absence of changes in fluorescence emission and far-UV CD in both BγS and HγS shows that the interactions between the domains do not involve significant alterations in the tertiary interactions of the two proteins. What the structural reason for the difference in the domain interactions between γB and γS is, requires further investigation. One obvious possibility is the length or conformation of the linker peptide between the domains.

In contrast to γB-crystallin at acid pH where the folding intermediate (with the C-terminal domain unfolded and the N-terminal one still native) is accessible to thermodynamic and kinetic experiments [3,23,32,33], HγS obviously shows a more complex behavior. At low denaturant concentrations, deviations from linearity in the chevron plots clearly point to significant populations of kinetic intermediates [25], in spite of the fact that the equilibrium transitions obey the two-state N ⇔ U model. Similar observations were reported for intact protein S (PS) from *Myxococcus xanthus* which is a structural homolog of γB [16]. In contrast to HγS and its isolated domains, which all three show the roll-over effect, the domains of PS can be quantitatively described by the two-state model [34]. Further investigations are required in order to elucidate the detailed folding pathway of HγS.

Differences in stability are notoriously difficult to explain, because marginal deviations in local interactions of residues or folding motifs may

cause drastic shifts in the equilibrium transitions and their corresponding Gibbs standard free energies of stabilization [3,35,36]. For BγS-crystallin (as for BγB-crystallin), the full-length protein and its N-terminal domain hardly differ in their half-concentrations at which unfolding occurs; on the other hand BγS-C is destabilized. Given the differences in the codon usage for the two domains [37], this might suggest mutual 'chaperoning' of the domains during translation and domain folding. However, the fact that in the case of the human protein the stability of HγS-C exceeds the stability of HγS-N clearly contradicts this idea. The slight but significant difference in stability between BγS and its mutant lacking the disordered N-terminal extension (BγS-5) cannot be explained by an entropic contribution because the corresponding additive contributions to the native and denatured states compensate each other.

A common property observed for all seven γS-crystallin variants is the two-state character of their thermodynamic stability profiles. As has been documented, this holds for all modes of denaturation. In contrast, γB-crystallin shows independent domain folding, at least under certain conditions. Both proteins exhibit significant differences in the stabilities of their isolated domains. Based on these findings and the structural homology, a more complex mechanism would be obvious also in the case of γS. Supposedly, the reason for the simultaneous N ⇔ U transition of γS-crystallin is the closely similar stability of its isolated domains. In the case of γB-crystallin, at neutral pH, practically the same behavior is observed [32]; however, at pH 2.0 where the two domains show a significant difference in their net charge, the C-terminal domain is destabilized giving rise to an unfolding intermediate with the C-terminal domain unfolded and the N-terminal one still in its native conformation [23,24]. Similar to γB-crystallin, protein S, from *Myxococcus xanthus*, shows biphasic equilibrium transitions. Here, the very unstable C-terminal domain is stabilized mainly by domain interactions with its highly stable N-terminal counterpart, especially at acidic pH [38,39]. In contrast, the domains of γS-crystallin exhibit comparable stabilities at all pH values, leading to two-state unfolding of the intact molecule. Therefore, we conclude that domain interactions do not contribute significantly to the overall stability of γS-crystallin. This might be the cause for the decreased stability of γS-crystallin compared to γB-crystallin, where very strong hydrophobic domain interactions are assumed to be essential for the extreme stability of the protein [3,24,32,34].

5. Nomenclature

γB, γS, BγS, HγS	γB-crystallin, γS-crystallin of bovine (B) and human (H) origin, respectively
-N and -C	the N- and C-terminal domains of the proteins, BγS-5 to the truncated mutant of BγS lacking five N-terminal residues
CD	circular dichroism
DTT	dithiothreitol
GdmCl	guanidinium chloride

Acknowledgements

Work was supported by the Deutsche Forschungsgemeinschaft, the Fonds der Chemischen Industrie and the Biomed Program of the European Community (BMH4-98-3895). We thank Drs K. Zaiss and R. Seckler for fruitful discussions, and Dr R. Deutzmann for help in performing the mass spectrometry and Edman degradation experiments.

References

[1] S.M. Podos, M. Yanoff (Eds.), Textbook of Ophthalmology, vol. 3. Ch. 4.1, Gower Medical Publ., New York, London, 1992.
[2] C. Slingsby, B. Norledge, A. Simpson et al., X-Ray diffraction and structure of crystallins, Prog. Ret. Eye Res. 16 (1997) 3–29.
[3] R. Jaenicke, Stability and folding of domain proteins, Prog. Biophys Mol. Biol. 71 (1999) 155–241.
[4] J.J. Harding, M.J.C. Crabbe, The lens: development, proteins, metabolism and cataract, in: H. Dawson (Ed.)

The Eye, vol.1B, Academic Press, London, 1984, pp. 207–492.
[5] H.J. Aarts, N.H. Lubsen, J.G. Schoenmakers, Crystallin gene expression during rat lens development, Eur. J. Biochem. 183 (1989) 31–36.
[6] C.N. Nagineni, S.P. Bhat, Lens fiber cell differentiation and expression of crystallins in cocultures of human fetal epithelial cells and fibroblasts, Exp. Eye Res. 54 (1992) 193–200.
[7] W.W. de Jong, N.H. Lubsen, H.J. Kraft, Molecular evolution of the eye lens, Prog. Ret. Eye Res. 13 (1994) 391–442.
[8] Y. Quax-Jeuken, H.P.C. Driessen, J. Leunissen, W. Quax, W. de Jong, W.H. Bloemendal, βS-Crystallin: structure and evolution of a distinct member of the βγ superfamily, EMBO J. 4 (1985) 2597–2602.
[9] T. Chang, W.C. Chang, Cloning and sequencing of a carp βS-crystallin, Biochim. Biophys. Acta 910 (1987) 80–92.
[10] S. Zarina, A. Abbasi, Z.H. Zaidi, Primary structure of βS-crystallin from human lens, Biochem. J. 287 (1992) 377–381.
[11] J.B. Smith, Z. Yang, P. Lin, Z. Zaidi, A. Abbasi, P. Russell, The complete sequence of human lens gamma S-crystallin, Biochem. J. 307 (1995) 407–410.
[12] S. Zarina, C. Slingsby, R. Jaenicke, Z.H. Zaidi, H. Driessen, N. Srinivasan, 3D-Model and quaternary structure of the human eye lens protein γS-crystallin based on β- and γ-crystallin X-ray coordinates and ultracentrifugation, Prot. Sci. 3 (1994) 1840–1846.
[13] J.A. Thomson, R.J. Siezen, E.D. Kaplan, M. Messner, B. Chakrabarti, Comparative studies of βS-crystallins from human, bovine, rat and rabbit lenses, Curr. Eye Res. 8 (1989) 139–149.
[14] P.G. Cooper, J.A. Carver, J.A. Aquilina, G.B. Ralston, R.J. Truscott, A ^{1}H-NMR spectroscopic comparison of γS- and γB-crystallins, Exp. Eye Res. 59 (1994) 221–224.
[15] C.W. Liu, N. Asherie, A. Lomakin, J. Pande, O. Ogun, G.B. Benedek, Phase separation in aqueous solutions of lens γ-crystallins: special role of γS, Proc. Natl. Acad. Sci. USA 93 (1996) 377–382.
[16] G. Wistow, Evolution of a protein superfamily: relationships between vertebrate lens crystallins and microorganism dormancy proteins, J. Mol. Evol. 30 (1990) 140–145.
[17] A.K. Basak, R.C. Kroone, N.H. Lubsen, C.E. Naylor, R. Jaenicke, C. Slingsby, The C-terminal domains of γS-crystallin pair about a distorted two-fold axis, Prot. Eng. 11 (1998) 337–344.
[18] S.C. Gill, P.H. von Hippel, Calculation of protein extinction coefficients from amino acid sequence data, Anal. Biochem. 182 (1989) 319–326.
[19] C.N. Pace, F. Vajdos, L. Fee, G. Grimsley, T. Gray, How to measure and predict the molar absorption coefficient of a protein, Prot. Sci. 4 (1995) 2411–2423.
[20] D.A. Yphantis, Equilibrium ultracentrifugation of dilute solutions, Biochemistry 3 (1964) 297–317.
[21] G.P. Privalov, V. Kavina, E. Freire, P.L. Privalov, Precise scanning calorimeter for study of thermal properties of biological macromolecules in dilute solutions, Anal. Biochem. 232 (1995) 79–85.
[22] R. Jaenicke, Folding and association of proteins, Prog. Biophys. Mol. Biol. 49 (1987) 117–237.
[23] R. Rudolph, R. Siebendritt, G. Neßlauer, A.K. Sharma, R. Jaenicke, Folding of an all-β protein, Independent domain folding in γII-crystallin from calf eye lens, Proc. Natl. Acad. Sci. USA 87 (1990) 4625–4629.
[24] E.M. Mayr, R. Jaenicke, R. Glockshuber, The domains in γB-crystallin: identical fold-different stabilities, J. Mol. Biol. 269 (1997) 260–269.
[25] R.L. Baldwin, On-pathway versus off-pathway folding intermediates, Folding Des. 1 (1996) R1–R8.
[26] F.X. Schmid, Kinetics of unfolding and refolding of single domain proteins, Protein Folding, in: T.E. Creighton (Ed.), Freeman, New York, 1992, pp. 197–241.
[27] P. Stiuso, R. Ragone, G. Colonna, Molecular organization and structural stability of βS-crystallin from calf lens, Biochemistry 29 (1990) 3929–3936.
[28] T.L. Blundell, P. Lindley, L. Miller et al., The molecular structure and stability of the eye lens: X-ray analysis of γ-crystallin II, Nature 289 (1981) 771–777.
[29] B. Bax, R. Lapatto, V. Nalini et al., X-Ray analysis of βB2-crystallin and evolution of oligomeric lens proteins, Nature 347 (1990) 776–780.
[30] B.V. Norledge, E.M. Mayr, R. Glockshuber et al., The X-ray structures of two mutant crystallin domains shed light on the evolution of multidomain proteins, Nat. Struct. Biol. 3 (1996) 267–274.
[31] B.V. Norledge, S. Trinkl, R. Jaenicke, C. Slingsby, The X-ray structure of a mutant eye lens βB2-crystallin with truncated sequence extensions, Prot. Sci. 6 (1997) 1612–1620.
[32] S. Palme, C. Slingsby, R. Jaenicke, Mutational analysis of hydrophobic domain interactions in γB crystallin from bovine eye lens, Prot. Sci. 6 (1997) 1529–1536.
[33] S. Palme, R. Jaenicke, C. Slingsby, X-Ray structures of three interface mutants of γB-crystallin from bovine eye lens, Prot. Sci. 7 (1998) 611–618.
[34] M. Wenk, R. Jaenicke, E.M. Mayr, Kinetic stabilisation of a modular protein by domain interactions, FEBS Lett. 438 (1998) 127–130.
[35] R. Jaenicke, Protein stability and molecular adaptation to extreme conditions, Eur. J. Biochem. 202 (1991) 715–728.
[36] R. Jaenicke, G. Böhm, Stabilization of proteins: what extremophiles teach us about protein stability, Curr. Opin. Struct. Biol. 8 (1998) 738–748.
[37] A.A. Komar, R. Jaenicke, Kinetics of translation of γ-crystallin and its circularly permuted variant in an in vitro cell-free system: possible relations to codon dis-

tribution and protein folding, FEBS Lett. 376 (1995) 195–198.

[38] M. Wenk, R. Baumgartner, T.A. Holak, R. Huber, R. Jaenicke, E.M. Mayr, The domains of protein S from *Myxococcus xanthus*: structure, stability and interactions, J. Mol. Biol. 286 (1999) 1533–1545.

[39] M. Wenk, R. Jaenicke, Calorimetric analysis of the Ca^{2+}-binding βγ-crystallin homolog protein S from *Myxococcus xanthus*: intrinsic stability and mutual stabilization of domains, J. Mol. Biol. 293 (1999) 117–124.